AAV9-NPC1 significantly ameliorates Purkinje cell death and behavioral abnormalities in mouse NPC disease[s]

Chang Xie,[1,*,†] Xue-Min Gong,[1,†] Jie Luo,* Bo-Liang Li,† and Bao-Liang Song[2,*]

Hubei Key Laboratory of Cell Homeostasis,* College of Life Sciences, Institute for Advanced Studies, Wuhan University, Wuhan 430072, China; and Institute of Biochemistry and Cell Biology,† Shanghai Institutes for Biological Sciences, Chinese Academy of Sciences, Shanghai 200031, China

ORCID ID: 0000-0002-7643-5321 (C.X.)

Abstract Niemann-Pick type C (NPC) disease is a fatal inherited neurodegenerative disorder caused by loss-of-function mutations in the *NPC1* or *NPC2* gene. There is no effective way to treat NPC disease. In this study, we used adeno-associated virus (AAV) serotype 9 (AAV9) to deliver a functional *NPC1* gene systemically into *NPC1*$^{-/-}$ mice at postnatal day 4. One single AAV9-NPC1 injection resulted in robust NPC1 expression in various tissues, including brain, heart, and lung. Strikingly, AAV9-mediated NPC1 delivery significantly promoted Purkinje cell survival, restored locomotor activity and coordination, and increased the lifespan of *NPC1*$^{-/-}$ mice. Our work suggests that AAV-based gene therapy is a promising means to treat NPC disease.—Xie, C., X-M. Gong, J. Luo, B-L. Li, and B-L. Song. **AAV9-NPC1 significantly ameliorates Purkinje cell death and behavioral abnormalities in mouse NPC disease.** *J. Lipid Res.* 2017. **58: 512–518.**

Supplementary key words cholesterol • gene therapy • Niemann-Pick type C disease • lysosomal storage diseases • adeno-associated virus serotype 9 • Niemann-Pick type C1 • blood-brain barrier

Niemann-Pick type C (NPC) disease is an autosomal recessive lysosomal storage disorder that primarily strikes children with featured symptoms such as cerebellar ataxia, dementia, dysphagia, dysarthria, hepatosplenomegaly, and premature death early in life. It results from loss-of-function mutations in *NPC1* (95% of cases) or *NPC2* (5% of cases), which encode a large polytopic membrane protein and a small luminal protein, respectively (1–3). In the lysosome, NPC2 binds and delivers LDL-derived cholesterol to the N-terminal domain of NPC1 (4). The NPC1-bound cholesterol then penetrates through the glycocalyx and inserts into the lysosomal membrane (4, 5). Deficiency in NPC1 or NPC2 impedes the egress of cholesterol out of the lysosome and, consequently, leads to NPC disease.

The current available therapies for NPC disease include miglustat, a glucosylceramide synthase inhibitor, and 2-hydroxypropyl-β-cyclodextrin, a cyclic oligosaccharide that binds and enhances the water solubility of cholesterol (6).These two compounds can effectively delay the onset of neurological signs, ameliorate cerebellar and liver dysfunction, and prolong the lifespan in the murine and feline models of NPC disease (7–10). Unfortunately, adverse side effects, such as outer hair cell death and hearing loss, inevitably follow 2-hydroxypropyl-β-cyclodextrin administration in a dose- and duration-dependent manner (10, 11). It is thus urgent to find other safe and efficacious alternatives to treat NPC disease.

Previous transgenic studies have shown that expressing WT NPC1 protein under a prion promoter (12) or neuron- and glial-specific promoters (13–15) is sufficient to prevent neurodegeneration and extend the lifespan of *NPC1*$^{-/-}$ mice, shedding light on a utilization of gene therapy to treat NPC disease. Notably, adeno-associated virus (AAV) has been widely adopted as an efficient and safe gene transfer tool to specifically deliver and express transgenes or components of other systems (such as CRISPR/Cas9) in various organs, including the liver, heart, and muscles (16–20). Among all serotypes, AAV serotype 9 (AAV9) can mediate gene expression in the brain and peripheral tissues following intravenous administration (21). Therefore, it is tempting to speculate that AAV9-mediated *NPC1* delivery may serve as a potential means to mitigate the neurodegenerative manifestations of NPC disease. However, the large

Abbreviations: AAV, adeno-associated virus; AAV9, adeno-associated virus serotype 9; NPC, Niemann-Pick type C; P4, postnatal day 4; PFA, paraformaldehyde; TBST, TBS containing 0.075% Tween-20.
[1] C. Xie and X-M. Gong contributed equally to this work.
[2] To whom correspondence should be addressed.
  e-mail: blsong@whu.edu.cn
[s] The online version of this article (available at http://www.jlr.org) contains a supplement.

(~3.9 kb) open reading frame poses a challenge to deliver a functional *NPC1* gene by AAV in vivo.

Here, we successfully packaged the expression cassette of NPC1 into a standard AAV9 vector. A single systemic injection of AAV9-NPC1 into $NPC1^{-/-}$ mice at postnatal day 4 (P4) resulted in high expression of NPC1 protein in the brain, lung, heart, and other peripheral tissues. Moreover, Purkinje cell survival, behavioral abnormalities, and lifespan were greatly improved in $NPC1^{-/-}$ mice following AAV9-NPC1 treatment. Together, our work establishes AAV9-mediated *NPC1* delivery as a novel and promising approach to treat NPC disease.

MATERIALS AND METHODS

Reagents

Hoechst (catalog number 63493) and filipin (catalog number F9765) were purchased from Sigma (St. Louis, MO). The total cholesterol assay kit (catalog number 20131112) was from Kehua Bio-engineering Co., Ltd. (Shanghai, China). Q5 high-fidelity DNA polymerase (catalog number M0491) was from New England BioLabs (Ipswich, MA).

Antibodies

The primary antibodies used were as follows: rabbit polyclonal anti-calnexin (catalog number 2433; Cell Signaling Technology, Danvers, MA); mouse monoclonal anti-clathrin heavy chain (catalog number 610499; BD Transduction Laboratories, San Jose, CA); mouse monoclonal anti-calbindin-D28K (catalog number C9848; Sigma); mouse monoclonal anti-Flag (catalog number F1804; Sigma); Alexa Fluor 555 goat anti-mouse IgG (1:500; catalog number A21422) and Alexa Fluor 488 goat anti-mouse IgG (1:500; catalog number A11001) were purchased from Life Technologies (Carlsbad, CA); horseradish peroxidase-conjugated goat anti-mouse (1:5,000; catalog number 31430) and anti-rabbit (1:5,000; catalog number 32460) IgG were purchased from Thermo Fisher Scientific (Waltham, MA).

Animals

All animal experiments were approved by the Biological Research Ethics Committee, Shanghai Institutes for Biological Sciences, Chinese Academy of Sciences. $NPC1^{-/-}$ and WT littermates were bred using heterozygous pairs (BALB/cNctr-Npc1m1N/J) purchased from the Jackson Laboratory (Bar Harbor, ME). Mice were fed on a chow diet ad libitum and housed in a pathogen-free animal facility in plastic cages at 22°C, with a daylight cycle from 6:00 AM to 6:00 PM. Pups were genotyped at 2 days of age. At 63 days of age, mice were subjected to the open field test and rotarod test.

Cells

CHO-7 and CT43 cells (generous gifts from Dr. Ta-Yuan Chang, Dartmouth Medical School, Hanover, NH) were grown in a monolayer at 37°C under 5% CO_2. Cells were maintained in the 1:1 mixture of Dulbecco's modified Eagle's medium and Ham's F-12 medium (DMEM/F-12; Invitrogen) containing 100 units/ml penicillin, 100 µg/ml streptomycin sulfate, and 5% FBS (Gibco). CHO-7 and CT43 cells were seeded at a density of 7×10^4 cells per well onto glass slides in 12-well plates (day 0). CT43 cells were transfected with 1 µg AAV-CMV-NPC1-miniPolyA plasmid (day 1). Twenty-four hours later (day 2), cells were fixed with 4% paraformaldehyde (PFA) and subjected to following staining processes (22).

Immunocytochemistry

Twenty-four hours after plasmid transfection, cells were fixed with 4% PFA in PBS for 30 min at room temperature and washed twice with PBS. Cells were incubated with 50 µg/ml filipin and 10 µg/ml anti-Flag antibody in the dark for 1 h, washed with PBS three times, and incubated with Alexa Fluor 488 goat anti-mouse IgG for 1 h at room temperature. Cells were examined and imaged under a Leica TCS SP5 confocal microscope.

Histochemistry

Mouse tissues were fixed in 4% PFA, embedded in paraffin, and cut into 3 µm sections using a microtome (Leica RM2235) or embedded in OCT for frozen section with a cryostat (Leica CM 3050S). For histological analysis, paraffin sections were deparaffinized and stained with H&E (Sigma). For immunostaining analysis, the sections were processed as previously described (23). Briefly, deparaffinized sections were boiled (95°C) for 15 min in 25 mM Tris-HCl and 1 mM EDTA buffer (pH 9.0) for antigen retrieval. The same procedures followed afterwards for both paraffin sections and frozen sections. Samples were then permeabilized and blocked with 5% FBS in PBS containing 0.5% Triton X-100 for 1 h at room temperature. Sections were incubated with primary antibodies overnight at 4°C and then washed with PBS three times followed by incubation with the appropriate secondary antibodies for 1 h at room temperature. Sections were finally incubated with 5 µg/ml Hoechst for 5 min and mounted.

Western blotting

Mouse tissues were snap-frozen and homogenized in 1 ml of RIPA buffer containing protease and phosphatase inhibitors with a high-throughput tissue homogenizer (Bertin Technologies; Precellys®24) as previously described (23, 24). Lysate was centrifuged at 10,000 g for 10 min at 4°C and protein concentrations were determined using the Lowry method (Bio-Rad). Samples were mixed with the loading buffer and boiled for 10 min. Proteins were resolved by SDS-PAGE electrophoresis and transferred onto nitrocellulose membranes. Membranes were blocked with 5% BSA in TBS containing 0.075% Tween-20 (TBST) and probed with primary antibodies overnight at 4°C. After washing in TBST three times, blots were incubated with secondary antibodies for 1 h at room temperature followed by three more washes in TBST. Immunoblots were analyzed with a Tanon 5200 chemiluminescent imaging system (Shanghai China).

AAV9-mediated gene expression

The coding region of mouse *NPC1* was cloned into the p3×Flag-CMV-14 vector. The NPC1-3×Flag sequence was then subcloned into a pAOV-CMV-minipolyA vector, as previously described (20). AAV9-EGFP and AAV9-NPC1 were prepared by Obio Technology Co., Ltd. (Shanghai, China).

P4 mice were anesthetized on wet ice. A total volume of 25 µl containing 2.5×10^{11} vg AAV9-EGFP or AAV9-NPC1 viruses was intracardially injected into the left ventricle using a 29 gauge insulin syringe (Ultral fine needle; BD). Mouse tissues were collected for Western blotting and histochemical analysis 8 weeks postinjection.

Open field test

A 40 cm × 40 cm field was equally divided into 3 × 3 squares with the middle square designated as the center. Mice dotted with crystal violet staining solution on their back were put onto the middle

of a piece of white paper covering the entire field and allowed to explore freely for 10 min. The movement was recorded by an overhead camera and the total distance traveled and time spent in the center were analyzed using EthoVision XT 10 (Noldus, Leesburg, VA).

Rotarod test

The balance and motor coordination of mice were tested on a rotarod machine (ZB_200; Chengdu Techman Software Co., Ltd.) as previously described (25).

Statistics

Results are presented as mean ± SD. All the data were analyzed by unpaired two-tailed Student's *t*-test or one-way ANOVA. Statistical significance was set at $P < 0.05$.

RESULTS

Generation of AAV9-based *NPC1* construct

To engineer a NPC1 expression cassette that would fit the packaging capacity (∼4.5–5.0 kb) of AAV9 vector, we employed a small-sized (664 bp) CMV promoter with high transcription activity NPC1 coding sequence fused with 3×Flag instead of fluorescent protein at the C terminus, and a 48 bp miniature poly(A) signal, rather than the commonly used hGH poly(A) signal (∼500 bp). The final CMV-NPC1-3×Flag-miniPolyA vector was 4.74 kb in size and appropriate for AAV9 packaging (**Fig. 1A**).

We next sought to test whether the *NPC1*-3×Flag construct would express a functional NPC1 protein. CT43 cells are deficient in NPC1 and display excess cholesterol in lysosomes (26). Overexpression of NPC1-3×Flag, however,

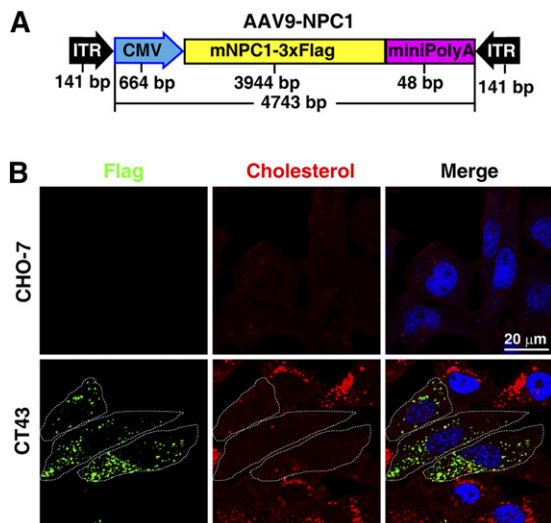substantially diminished lysosomal cholesterol to an extent found in WT CHO-7 cells, whereas neighboring untransfected cells still exhibited robust filipin staining (Fig. 1B). These results suggest that ectopic NPC1 expression successfully rectifies *NPC1*-deficient-related cholesterol accumulation in vitro.

We then incorporated NPC1-3×Flag into a standard AAV9 vector and intracardially injected AAV9-NPC1 into the heart of $NPC1^{-/-}$ mice at P4. Each mouse received a single injection of 25 µl containing 2.5×10^{11} vg of virus, and the expression levels of NPC1 in different tissues were analyzed 2 months postinjection. The validity and specificity of M2 anti-Flag antibody was confirmed (supplemental Fig.
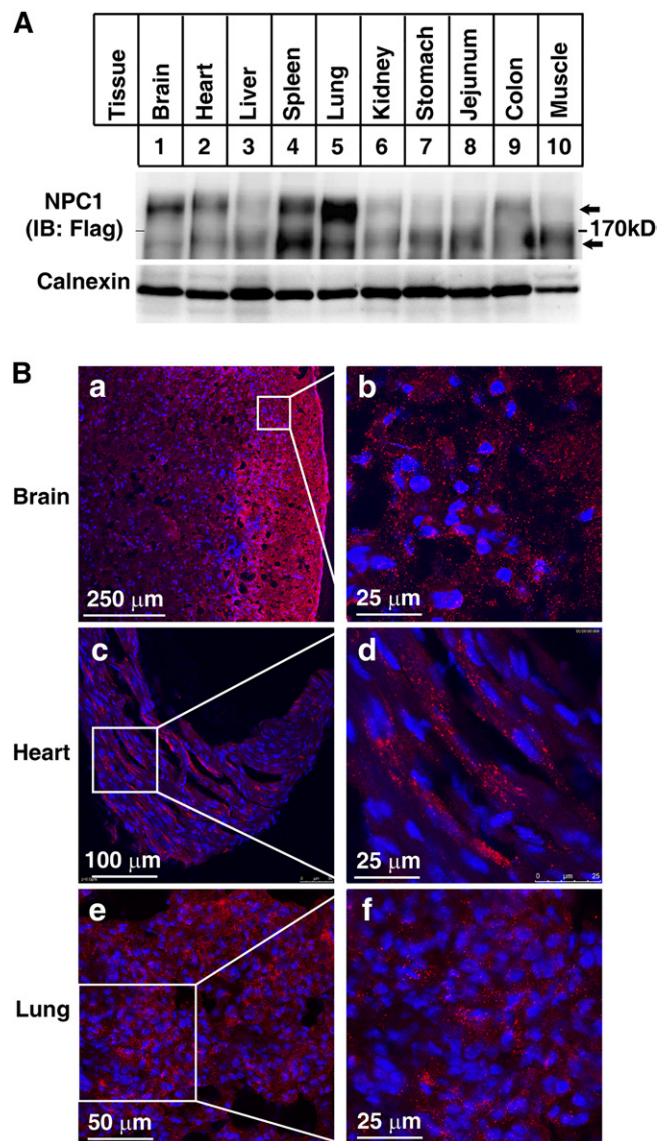
Fig. 1. Construction of an AAV9-based plasmid expressing the functional NPC1 protein. A: Diagram of the AAV9 vector expressing NPC1-3×Flag. B: Expression of exogenous NPC1 attenuates lysosomal cholesterol accumulation in CT43 cells. CT43 cells were transfected with AAV9-NPC1-3×Flag. Cholesterol and NPC1 protein were visualized by filipin staining (pseudocolored red) and the anti-Flag antibody (pseudocolored green), respectively. Nuclei were stained with SYBGreen (pseudocolored blue). Scale bar, 20 µm.

Fig. 2. Intracardiac injection of AAV9-NPC1 delivers widespread expression of NPC1 in various tissues. A: Expression profiles of AAV9-delivered NPC1 in the indicated tissues of $NPC1^{-/-}$ mice 2 months postinjection. Calnexin is used as a loading control. B: Confocal images of exogenous NPC1 staining (red) in the brain, heart, and lung. Nuclei were counterstained with Hoechst (blue). Boxed areas in the left column are shown at a higher magnification in the right column.
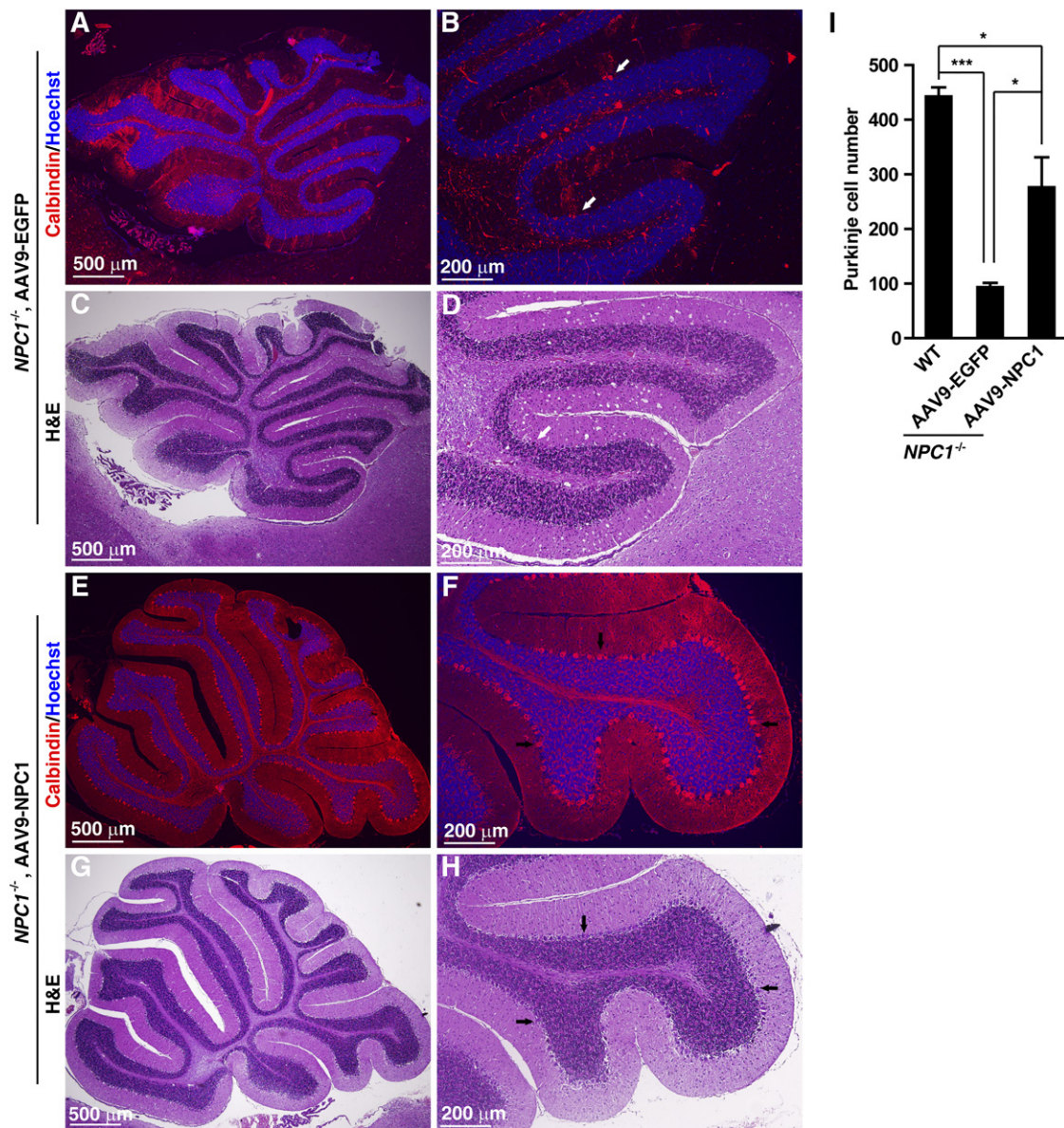
Fig. 3. Intracardiac injection of AAV9-NPC1 improves the survival of Purkinje cells in $NPC1^{-/-}$ mice. A, B, E, F: Representative images of calbindin-positive (red) cerebellar Purkinje cells of $NPC1^{-/-}$ mice injected with AAV9-EGFP (A, B) or AAV9-NPC1 (E, F). Nuclei were counterstained with Hoechst (blue). C, D, G, H: H&E staining showing cerebellar Purkinje cells of $NPC1^{-/-}$ mice injected with AAV9-EGFP (C, D) or AAV9-NPC1 (G, H). Images on the left are shown at a higher magnification than on the right. Arrows indicate individual Purkinje cells. I: Purkinje cell numbers counted from cerebellar sections (n = 5, 3, and 5 for WT, AAV9-EGFP, and AAV9-NPC1, respectively). Unpaired two-tailed Student's t-test; $*P < 0.05$, $***P < 0.001$.

S2). High levels of mature glycosylated NPC1 expression were evident in the lung, brain, heart, and spleen, followed by less robust, but still apparent, signal in the liver, kidney, and colon (**Fig. 2A**). A minimal amount of NPC1 was present in the stomach, jejunum, and muscle (Fig. 2A). Immunohistochemical analysis revealed that AAV9-delivered NPC1 primarily localized in the outer cerebral cortex, whereas the distribution of NPC1 expression was relatively homogeneous throughout the heart and lung (Fig. 2B). A similar pattern was also observed following AAV9-EGFP injection (supplemental Fig. S1A, B), suggesting that the delivery method, but not exogenous protein per se, determines distributions of the proteins. Importantly, ectopic NPC1 appeared to form cytoplasmic puncta and correspond to

lysosome patterning in the cells of the abovementioned tissues.

AAV9-NPC1 injection dramatically improves the survival of Purkinje cells

Purkinje cell loss, which initiates from 49 days of age and becomes pronounced by 9 weeks of age in $NPC1^{-/-}$ mice, is a hallmark of NPC disease (10, 27, 28). To evaluate the effect of AAV9-NPC1 injection on Purkinje cell survival, we administered AAV9-EGFP or AAV9-NPC1 systemically into $NPC1^{-/-}$ mice at P4 and examined cerebellar Purkinje cells 2 months postinjection. A severe loss of Purkinje cells was observed in $NPC1^{-/-}$ mice injected with AAV9-EGFP (**Fig. 3A–D**). AAV9-NPC1 treatment, however, significantly

improved Purkinje cell survival, as revealed by calbindin labeling (Fig. 3E, F) and H&E staining (Fig. 3G, H). Quantification showed that the number of Purkinje cells increased by about 160% in AAV9-NPC1-injected mice compared with that of AAV9-EGFP-injected mice (Fig. 3I).

AAV9-NPC1 injection rescued the gene expression abnormalities in liver and brain of $NPC1^{-/-}$ mice

Deficiency in NPC1 or NPC2 impedes the lysosome-to-ER transport of LDL-cholesterol; therefore, it activates the expression of the genes involved in cholesterol biosynthesis (7). In addition, a compensatory increase in lysosomal genes was observed due to lysosomal dysfunctions (9, 29). Inflammation was upregulated in NPC1-deficient mice. We then examined gene expression profiles of the abovementioned biological events. RT-quantitative (q)PCR revealed a significant decrease in the genes involved in cholesterol metabolism (*ApoB*, *HMGCS*), lysosome (*LIMP1*, *cathepsin L1*, *cathepsin B*, *acid lipase*), and inflammation (*TNFα*, *CCL5*) in the liver of $NPC1^{-/-}$ mice receiving AAV9-NPC1 injection compared with those receiving AAV9-EGFP injection (**Fig. 4A**). Similar effects were also observed in brain tissue (Fig. 4B).

AAV9-NPC1 injection significantly ameliorated the motor deficits of $NPC1^{-/-}$ mice

We next monitored the general activity and motor coordination of WT littermates and $NPC1^{-/-}$ mice injected with AAV9-EGFP or AAV9-NPC1 using the open field paradigm. $NPC1^{-/-}$ mice were less active and showed defects in moving, standing, and taking food at the age of 9 weeks (data not shown). Compared with WT controls that primarily moved marginally, $NPC1^{-/-}$ mice injected with AAV9-EGFP displayed a shorter moving distance with significantly longer periods in the center (**Fig. 5A–C**). These moving deficits, however, were markedly rescued by AAV9-NPC1 administration (Fig. 5A–C). When subjected to the rotarod test, AAV9-NPC1-treated mice stayed on top of a rotating cylinder for a much longer time than those receiving AAV9-EGFP (Fig. 5D). These results indicate that AAV9-NPC1 treatment effectively ameliorates the locomotor activity and motor coordination in $NPC1^{-/-}$ mice.

AAV9-NPC1 injection extended the lifespan of $NPC1^{-/-}$ mice

We finally assessed whether systemic AAV9-NPC1 injection could increase the survival time of $NPC1^{-/-}$ mice. AAV9-EGFP-injected mice usually died between 66 and 82 days of age (**Fig. 6**), comparable to untreated animals or those receiving saline (data not shown). AAV9-NPC1 administration significantly increased the average lifespan of $NPC1^{-/-}$ mice by 30% (AAV9-EGFP: 71 ± 4 days; AAV9-NPC1: 94 ± 4 days) (Fig. 6).

DISCUSSION

NPC disease is a neurodegenerative disorder with much more severe defects in the CNS than in the peripheral tissues (14, 30). Replacement expression of WT NPC1 transgene
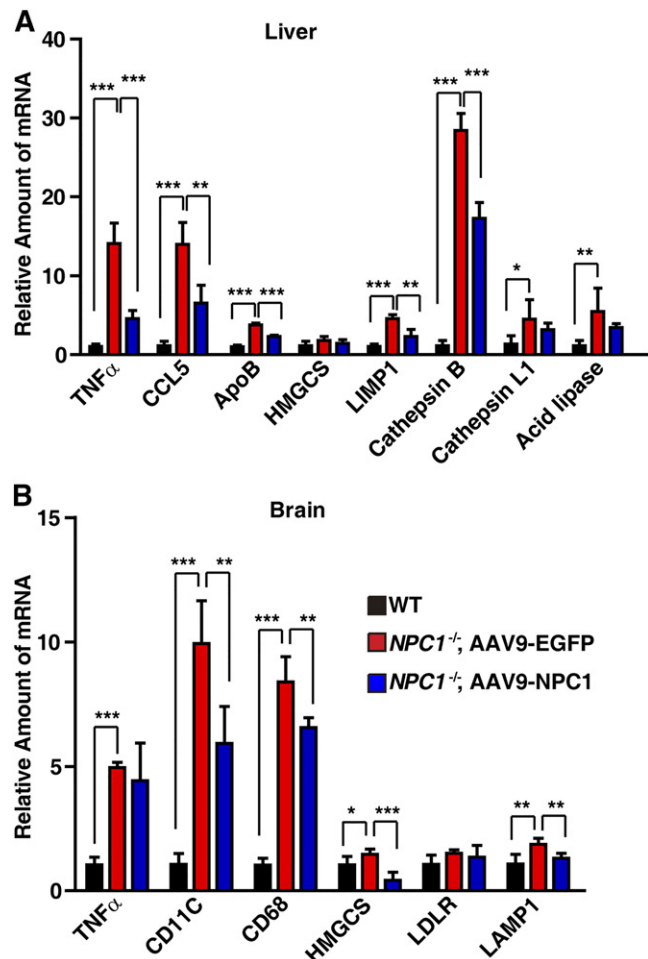

Fig. 4. Intracardiac injection of AAV9-NPC1 reverses expression of associated genes. A: Quantitative PCR analysis of genes in liver of WT mice and $NPC1^{-/-}$ mice injected with AAV9-EGFP or AAV9-NPC1. B: Quantitative PCR analysis of genes in brain of WT mice and $NPC1^{-/-}$ mice injected with AAV9-EGFP or AAV9-NPC1. Data are presented as mean ± SD; *$P < 0.05$, **$P < 0.01$, ***$P < 0.001$, unpaired two-tailed Student's *t*-test.

in neurons and astrocytes effectively corrects the neurological signs and prolongs the lifespan of $NPC1^{-/-}$ mice, suggesting an interesting possibility of re-expressing a functional NPC1 protein in the CNS by gene therapy to treat NPC disease.

An ideal gene therapy would correct the disease-causing mutations in every single cell. Although new powerful gene editing tools, such as TALEN and CRISPR/Cas9, are emerging, precise DNA repair is still difficult to achieve and only feasible in the zygotes and liver where highly efficient homologous recombination occurs (31–34). Because the direct DNA repair of mutant *NPC1* in the CNS is hardly approachable, we thus took the traditional gene therapy strategy to treat recessive inherited NPC disease by re-expressing functional copies of the target gene (16, 17).

Nevertheless, how to assure specific delivery and the stable long-term expression of transgenes remains challenging. Several vectors, such as adenovirus, lentivirus, and AAV, have been used for in vivo gene delivery. Lentivirus can integrate into the genomic DNA of target cells, but
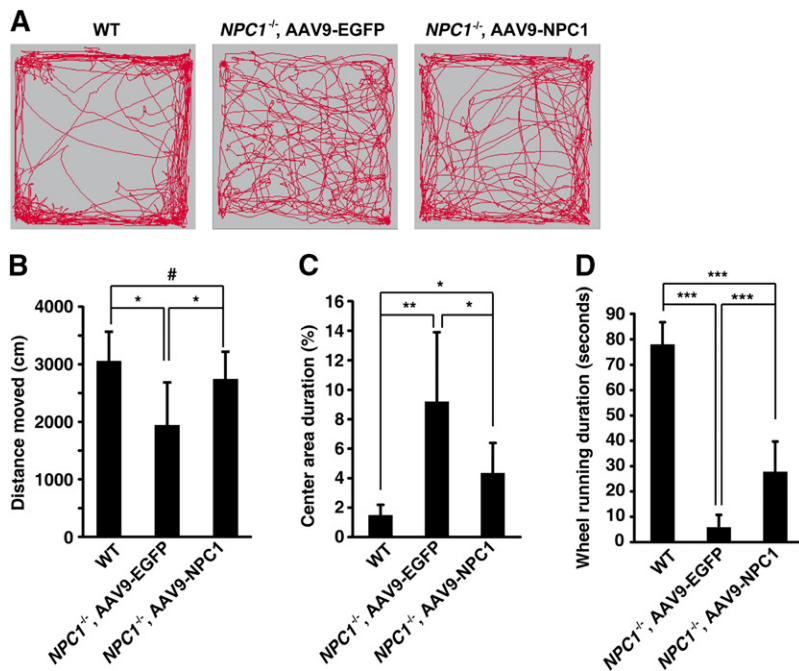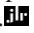
Fig. 5. Intracardiac injection of AAV9-NPC1 ameliorates motor impairments of $NPC1^{-/-}$ mice. A: Representative images showing typical travel pathways of WT mice and $NPC1^{-/-}$ mice injected with AAV9-EGFP or AAV9-NPC1 in the open field test. B: Total distance traveled in a 10 min test. C: Total time spent in the center of the open field. D: Average time spent on the rotarod. Data are presented as mean ± SD; n = 5 (WT), 7 (AAV9-EGFP), and 8 (AAV-NPC1). #$P > 0.05$, *$P < 0.05$, **$P < 0.01$, ***$P < 0.001$, one-way ANOVA.

induces insertional mutagenesis. Adenovirus, though non-integrative and safer, produces only transient expression (35). AAV, via different serotypes, transduces nondividing cells of various tissues and results in highly efficient gene expression without genome integration (16). AAV-mediated delivery of factor IX and LDLR, which were developed for therapeutic purposes for hemophilia B and homozygous familial hypercholesterolemia, respectively, is currently in phase 1 and phase 2 clinical trials (36–38). AAV9, owing to the capability of infecting both neurons and glial cells upon intravenous injection (21), is a good candidate for transferring the *NPC1* gene into the CNS of $NPC1^{-/-}$ mice.

In this study, the lifespan of $NPC1^{-/-}$ mice was increased by about 30% after a single intraventricular injection of AAV9-NPC1 at P4. This limited improvement is probably attributable to the restricted NPC1 expression in the outer cortex and hippocampus (supplemental Fig. S1B). We have also tried intracranial administration and found a widespread expression of NPC1 in both the cerebrum and cerebellum (supplemental Fig. S3A, B). This would be

more helpful to improve longevity. In addition, a very recent study reports that retro-orbital delivery of AAV9-based NPC1 expression under CamKII or EF1a promoters substantially increases the lifespan of $NPC1^{-/-}$ mice (39). It will be interesting to compare the effects of various delivering routes, such as intracisternal (40), intracerebroventricular (41), or intracranial injections, on NPC1 expression in the CNS, as well as the reparative effects of AAV9-NPC1 on NPC1 phenotypes. In addition, whether a combination of different types of AAVs efficiently promotes global gene delivery needs further investigation.

In summary, our study demonstrates that AAV9-delivered expression of NPC1 is an effective way to treat NPC disease.∎
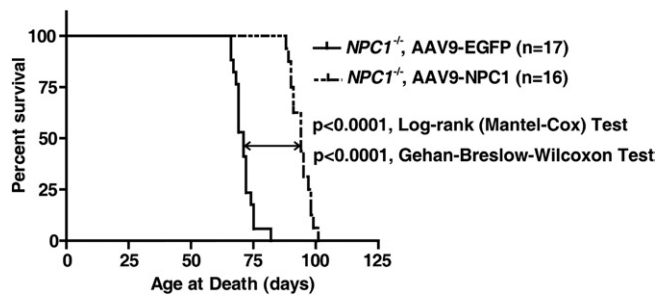
Fig. 6. Intracardiac injection of AAV9-NPC1 increases the lifespan of $NPC1^{-/-}$ mice. The lifespan of $NPC1^{-/-}$ mice injected with AAV9-EGFP or AAV9-NPC1 at P4 [n = 17 (AAV9-EGFP) and 16 (AAV9-NPC1)]. *P* values were generated by Log-rank (Mantel-Cox) test and Gehan-Breslow-Wilcoxon test.

REFERENCES

1. Carstea, E. D., J. A. Morris, K. G. Coleman, S. K. Loftus, D. Zhang, C. Cummings, J. Gu, M. A. Rosenfeld, W. J. Pavan, D. B. Krizman, et al. 1997. Niemann-Pick C1 disease gene: homology to mediators of cholesterol homeostasis. *Science.* **277:** 228–231.
2. Loftus, S. K., J. A. Morris, E. D. Carstea, J. Z. Gu, C. Cummings, A. Brown, J. Ellison, K. Ohno, M. A. Rosenfeld, D. A. Tagle, et al. 1997. Murine model of Niemann-Pick C disease: mutation in a cholesterol homeostasis gene. *Science.* **277:** 232–235.
3. Naureckiene, S., D. E. Sleat, H. Lackland, A. Fensom, M. T. Vanier, R. Wattiaux, M. Jadot, and P. Lobel. 2000. Identification of HE1 as the second gene of Niemann-Pick C disease. *Science.* **290:** 2298–2301.
4. Wang, M. L., M. Motamed, R. E. Infante, L. Abi-Mosleh, H. J. Kwon, M. S. Brown, and J. L. Goldstein. 2010. Identification of surface residues on Niemann-Pick C2 essential for hydrophobic handoff of cholesterol to NPC1 in lysosomes. *Cell Metab.* **12:** 166–173.
5. Kwon, H. J., L. Abi-Mosleh, M. L. Wang, J. Deisenhofer, J. L. Goldstein, M. S. Brown, and R. E. Infante. 2009. Structure of

N-terminal domain of NPC1 reveals distinct subdomains for binding and transfer of cholesterol. *Cell.* **137:** 1213–1224.

6. Liu, B. 2012. Therapeutic potential of cyclodextrins in the treatment of Niemann-Pick type C disease. *Clin. Lipidol.* **7:** 289–301.

7. Abi-Mosleh, L., R. E. Infante, A. Radhakrishnan, J. L. Goldstein, and M. S. Brown. 2009. Cyclodextrin overcomes deficient lysosome-to-endoplasmic reticulum transport of cholesterol in Niemann-Pick type C cells. *Proc. Natl. Acad. Sci. USA.* **106:** 19316–19321.

8. Liu, B., C. M. Ramirez, A. M. Miller, J. J. Repa, S. D. Turley, and J. M. Dietschy. 2010. Cyclodextrin overcomes the transport defect in nearly every organ of NPC1 mice leading to excretion of sequestered cholesterol as bile acid. *J. Lipid Res.* **51:** 933–944.

9. Liu, B., S. D. Turley, D. K. Burns, A. M. Miller, J. J. Repa, and J. M. Dietschy. 2009. Reversal of defective lysosomal transport in NPC disease ameliorates liver dysfunction and neurodegeneration in the npc1-/- mouse. *Proc. Natl. Acad. Sci. USA.* **106:** 2377–2382.

10. Vite, C. H., J. H. Bagel, G. P. Swain, M. Prociuk, T. U. Sikora, V. M. Stein, P. O'Donnell, T. Ruane, S. Ward, A. Crooks, et al. 2015. Intracisternal cyclodextrin prevents cerebellar dysfunction and Purkinje cell death in feline Niemann-Pick type C1 disease. *Sci. Transl. Med.* **7:** 276ra26.

11. Crumling, M. A., L. Liu, P. V. Thomas, J. Benson, A. Kanicki, L. Kabara, K. Halsey, D. Dolan, and R. K. Duncan. 2012. Hearing loss and hair cell death in mice given the cholesterol-chelating agent hydroxypropyl-beta-cyclodextrin. *PLoS One.* **7:** e53280.

12. Loftus, S. K., R. P. Erickson, S. U. Walkley, M. A. Bryant, A. Incao, R. A. Heidenreich, and W. J. Pavan. 2002. Rescue of neurodegeneration in Niemann-Pick C mice by a prion-promoter-driven Npc1 cDNA transgene. *Hum. Mol. Genet.* **11:** 3107–3114.

13. Lopez, M. E., A. D. Klein, U. J. Dimbil, and M. P. Scott. 2011. Anatomically defined neuron-based rescue of neurodegenerative Niemann-Pick type C disorder. *J. Neurosci.* **31:** 4367–4378.

14. Borbon, I., J. Totenhagen, M. T. Fiorenza, S. Canterini, W. Ke, T. Trouard, and R. P. Erickson. 2012. Niemann-Pick C1 mice, a model of "juvenile Alzheimer's disease", with normal gene expression in neurons and fibrillary astrocytes show long term survival and delayed neurodegeneration. *J. Alzheimers Dis.* **30:** 875–887.

15. Zhang, M., D. Strnatka, C. Donohue, J. L. Hallows, I. Vincent, and R. P. Erickson. 2008. Astrocyte-only Npc1 reduces neuronal cholesterol and triples life span of Npc1-/- mice. *J. Neurosci. Res.* **86:** 2848–2856.

16. Daya, S., and K. I. Berns. 2008. Gene therapy using adeno-associated virus vectors. *Clin. Microbiol. Rev.* **21:** 583–593.

17. Mueller, C., and T. R. Flotte. 2008. Clinical gene therapy using recombinant adeno-associated virus vectors. *Gene Ther.* **15:** 858–863.

18. Blankinship, M. J., P. Gregorevic, and J. S. Chamberlain. 2006. Gene therapy strategies for Duchenne muscular dystrophy utilizing recombinant adeno-associated virus vectors. *Mol. Ther.* **13:** 241–249.

19. Nathwani, A. C., E. G. Tuddenham, S. Rangarajan, C. Rosales, J. McIntosh, D. C. Linch, P. Chowdary, A. Riddell, A. J. Pie, C. Harrington, et al. 2011. Adenovirus-associated virus vector-mediated gene transfer in hemophilia B. *N. Engl. J. Med.* **365:** 2357–2365.

20. Xie, C., Y. P. Zhang, L. Song, J. Luo, W. Qi, J. Hu, D. Lu, Z. Yang, J. Zhang, J. Xiao, et al. 2016. Genome editing with CRISPR/Cas9 in postnatal mice corrects PRKAG2 cardiac syndrome. *Cell Res.* **26:** 1099–1111.

21. Foust, K. D., X. Wang, V. L. McGovern, L. Braun, A. K. Bevan, A. M. Haidet, T. T. Le, P. R. Morales, M. M. Rich, A. H. Burghes, et al. 2010. Rescue of the spinal muscular atrophy phenotype in a mouse model by early postnatal delivery of SMN. *Nat. Biotechnol.* **28:** 271–274.

22. Chu, B. B., Y. C. Liao, W. Qi, C. Xie, X. Du, J. Wang, H. Yang, H. H. Miao, B. L. Li, and B. L. Song. 2015. Cholesterol transport through lysosome-peroxisome membrane contacts. *Cell.* **161:** 291–306.

23. Xie, C., Z. S. Zhou, N. Li, Y. Bian, Y. J. Wang, L. J. Wang, B. L. Li, and B. L. Song. 2012. Ezetimibe blocks the internalization of NPC1L1 and cholesterol in mouse small intestine. *J. Lipid Res.* **53:** 2092–2101.

24. Ge, L., J. Wang, W. Qi, H. H. Miao, J. Cao, Y. X. Qu, B. L. Li, and B. L. Song. 2008. The cholesterol absorption inhibitor ezetimibe acts by blocking the sterol-induced internalization of NPC1L1. *Cell Metab.* **7:** 508–519.

25. Jones, B. J., and D. J. Roberts. 1968. The quantitative measurement of motor inco-ordination in naive mice using an acelerating rotarod. *J. Pharm. Pharmacol.* **20:** 302–304.

26. Cadigan, K. M., D. M. Spillane, and T. Y. Chang. 1990. Isolation and characterization of Chinese hamster ovary cell mutants defective in intracellular low density lipoprotein-cholesterol trafficking. *J. Cell Biol.* **110:** 295–308.

27. Ko, D. C., L. Milenkovic, S. M. Beier, H. Manuel, J. Buchanan, and M. P. Scott. 2005. Cell-autonomous death of cerebellar Purkinje neurons with autophagy in Niemann-Pick type C disease. *PLoS Genet.* **1:** 81–95.

28. Buard, I., and F. W. Pfrieger. 2014. Relevance of neuronal and glial NPC1 for synaptic input to cerebellar Purkinje cells. *Mol. Cell. Neurosci.* **61:** 65–71.

29. Xie, X., M. S. Brown, J. M. Shelton, J. A. Richardson, J. L. Goldstein, and G. Liang. 2011. Amino acid substitution in NPC1 that abolishes cholesterol binding reproduces phenotype of complete NPC1 deficiency in mice. *Proc. Natl. Acad. Sci. USA.* **108:** 15330–15335.

30. Erickson, R. P. 2013. Current controversies in Niemann-Pick C1 disease: steroids or gangliosides; neurons or neurons and glia. *J. Appl. Genet.* **54:** 215–224.

31. Wu, Y., D. Liang, Y. Wang, M. Bai, W. Tang, S. Bao, Z. Yan, D. Li, and J. Li. 2013. Correction of a genetic disease in mouse via use of CRISPR-Cas9. *Cell Stem Cell.* **13:** 659–662.

32. Yang, Y., L. Wang, P. Bell, D. McMenamin, Z. He, J. White, H. Yu, C. Xu, H. Morizono, K. Musunuru, et al. 2016. A dual AAV system enables the Cas9-mediated correction of a metabolic liver disease in newborn mice. *Nat. Biotechnol.* **34:** 334–338.

33. Yin, H., W. Xue, S. Chen, R. L. Bogorad, E. Benedetti, M. Grompe, V. Koteliansky, P. A. Sharp, T. Jacks, and D. G. Anderson. 2014. Genome editing with Cas9 in adult mice corrects a disease mutation and phenotype. *Nat. Biotechnol.* **32:** 551–553.

34. Long, C., J. R. McAnally, J. M. Shelton, A. A. Mireault, R. Bassel-Duby, and E. N. Olson. 2014. Prevention of muscular dystrophy in mice by CRISPR/Cas9-mediated editing of germline DNA. *Science.* **345:** 1184–1188.

35. Nász, I., and E. Adam. 2001. Recombinant adenovirus vectors for gene therapy and clinical trials. *Acta Microbiol. Immunol. Hung.* **48:** 323–348.

36. Ajufo, E., and M. Cuchel. 2016. Recent developments in gene therapy for homozygous familial hypercholesterolemia. *Curr. Atheroscler. Rep.* **18:** 22.

37. George, L. A., and P. F. Fogarty. 2016. Gene therapy for hemophilia: past, present and future. *Semin. Hematol.* **53:** 46–54.

38. Brimble, M. A., U. M. Reiss, A. C. Nathwani, and A. M. Davidoff. 2016. New and improved AAVenues: current status of hemophilia B gene therapy. *Expert Opin. Biol. Ther.* **16:** 79–92.

39. Chandler, R. J., I. M. Williams, A. L. Gibson, C. D. Davidson, A. A. Incao, B. T. Hubbard, F. D. Porter, W. J. Pavan, and C. P. Venditti. 2016. Systemic AAV9 gene therapy improves the lifespan of mice with Niemann-Pick disease, type C1. *Hum. Mol. Genet.* Epub ahead of print. October 25, 2016; doi:10.1093/hmg/ddw367.

40. Bucher, T., M. A. Colle, E. Wakeling, L. Dubreil, J. Fyfe, D. Briot-Nivard, M. Maquigneau, S. Raoul, Y. Cherel, S. Astord, et al. 2013. scAAV9 intracisternal delivery results in efficient gene transfer to the central nervous system of a feline model of motor neuron disease. *Hum. Gene Ther.* **24:** 670–682.

41. Dirren, E., C. L. Towne, V. Setola, D. E. Redmond, Jr., B. L. Schneider, and P. Aebischer. 2014. Intracerebroventricular injection of adeno-associated virus 6 and 9 vectors for cell type-specific transgene expression in the spinal cord. *Hum. Gene Ther.* **25:** 109–120.